

Measurement of Rare Kaon Decay $K^+ \rightarrow \pi^+ \nu \bar{\nu}$

Shaomin Chen

*TRIUMF, 4004 Wesbrook Mall, Vancouver,
B.C., V6T 2A3, Canada*

A decade long search for the rare kaon decay to $\pi^+ \nu \bar{\nu}$ has been pursued by E787. Two signal events are observed, giving a measurement of the branching ratio $\text{Br}(K^+ \rightarrow \pi^+ \nu \bar{\nu}) = 1.57_{-0.82}^{+1.75} \times 10^{-10}$ and a constraint on the Cabibbo-Kobayashi-Maskawa (CKM) matrix element $0.007 < |V_{td}| < 0.030$ (68% C.L.).

1 Introduction

In the Standard Model (SM) the transition K^+ to $\pi^+ \nu \bar{\nu}$ is a Flavor Changing Neutral Current (FCNC) process in which the first order weak decay is forbidden by the GIM mechanism but is allowed, though highly suppressed, in second order due to the differing masses of the up, charm and top quarks in the mediating loops. Theoretically, this decay is sensitive to the CKM matrix element V_{td} , which is one of two CKM matrix elements containing CP violation information in the SM. A study of this decay can provide a constraint on the range of V_{td} from the branching ratio of $K^+ \rightarrow \pi^+ \nu \bar{\nu}$. The SM predicts the branching ratio of this decay mode¹ to be $(0.72 \pm 0.21) \times 10^{-10}$ from a fit using $B_d - \bar{B}_d$ and $B_s - \bar{B}_s$ mixing and other relevant SM parameters. The theoretical uncertainty in $\text{Br}(K^+ \rightarrow \pi^+ \nu \bar{\nu})$ is small ($\sim 7\%$)², and long distance contributions to this decay are found to be negligible³. Therefore, a precise measurement can also serve as a probe for new physics beyond the SM. Most interestingly, this decay together with the neutral kaon decay $K_L \rightarrow \pi^0 \nu \bar{\nu}$ and the third most accurately measured CKM matrix element V_{cb} can also form a unitarity triangle in the $\rho - \eta$ plane, thus providing an approach for understanding CP violation.

The E787 experiment at Brookhaven National Laboratory found the first candidate event in 1995 data⁴ and recently found the second candidate event in 1998 data⁵. This talk will present the final E787 analysis result using data produced from about 6×10^{12} charged kaons at the Alternating Gradient Synchrotron (AGS) accelerator.

2 The E787 Detector

The E787 experiment (see Figure 1) is designed to capture the signature of $K^+ \rightarrow \pi^+ \nu \bar{\nu}$, i.e., a charged kaon decay to a charged pion of momentum below 227 MeV/c and no other associated observable product. Potential background can be $K^+ \rightarrow \mu^+ \nu_\mu (\gamma)$ (due to μ^+ misidentified as π^+ or mismeasured kinematics or missed photon), $K^+ \rightarrow \pi^+ \pi^0$ (due to missed photon or mismeasured kinematics), beam backgrounds (due to incoming π^+ mis-identified as K^+ or π^+ faking K^+ decay at rest or K^+ decay in flight or two incoming beam particles), or charge exchange background (due to $K^+ n \rightarrow K^0 p$, $K_L^0 \rightarrow \pi^+ l^- \nu_l$). A detailed description of the E787

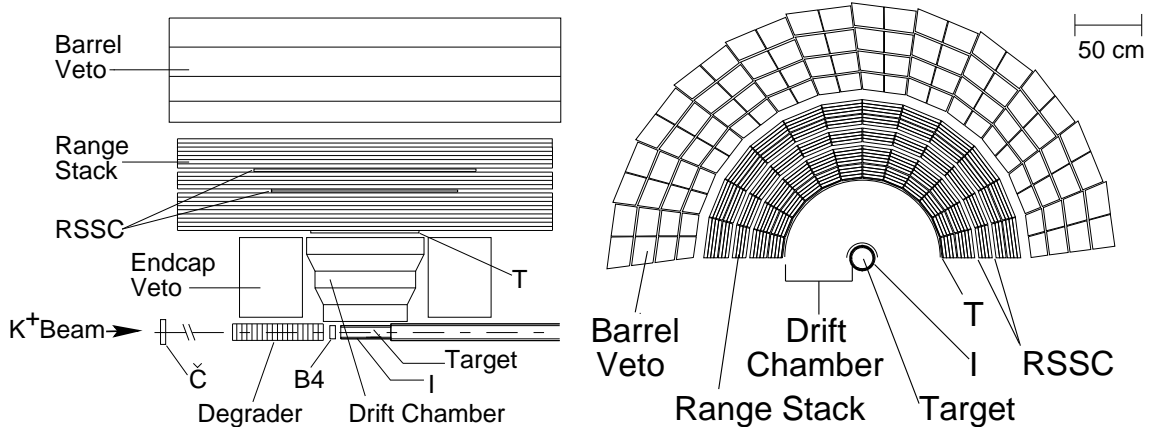


Figure 1: Top half of side (left) and end (right) views of the E787 detector.

detector can be found elsewhere⁶. The features relevant for this analysis are outlined in the following.

When 700-800 MeV/ c charged kaons with about 20% pion contamination are delivered to the E787 detector, they pass through a set of beam counters. The first of these is the threshold Čerenkov counter used to identify kaons and pions in the beam. The beam then passes through two beam wire chambers (BWPC) used for identifying multiple beam particles close to each other in space and time. The beam is slowed down by a degrader made of beryllium oxide followed by lead glass, the latter used for detecting pions in the beam or photons from kaon decay in the target. Located between the degrader and the target is a hodoscope (B4 counter) consisting of 2 planes of 8 scintillator fingers each, which provides dE/dx , position, and timing information for the incident kaon, as well as K/π separation and identification of possible two beam particles.

After passing through the beam counters, kaons are slowed down and finally stopped at the center of the detector through ionization energy loss in the target, which is made of 413 5-mm-square plastic scintillating fibers, each 310 cm long and connected to a phototube. Pulses from the phototubes are fed to ADCs, TDCs and 500-MHz CCD transient digitizers. The target detector can also be used to identify possible two beam particles, and to distinguish K^+ and π^+ using both time and energy measurements.

When a kaon stops and decays in the target, the daughter charged particle will pass through the I-counters, which consist of six scintillators in a ring surrounding the target. The time measurement from the I-counters together with the time measurement from the beam counters are used to form a delayed coincidence requirement in the online trigger which rejects prompt beam backgrounds.

After the I-counter, the charged particle is tracked by the Ultra Thin Chamber (UTC), which has 12 layers of anode wires for measuring the transverse momentum in the 1-T magnetic field. In addition to this, there are six foils etched with helical cathode strips providing a dip angle or z measurement in the $r-z$ plane. After correction for energy loss in the target and I-counter, the momentum resolution is measured to be $\sigma_P/P \sim 1.1\%$.

Upon exiting the UTC, the charged particle enters the range stack of plastic scintillators (RS), which consists of 21 radial layers in 24 azimuthal sectors. Each range stack module is instrumented with a phototube at each end. Pulses from these phototubes are delivered to ADCs and 500-MHz transient digitizers (TDs), thus providing kinetic energy and range measurements. Located after layer 10 and 14 are two layers of straw-tube tracking chambers (RSSCs), which provide position measurements of charged tracks in the RS. After making corrections for the

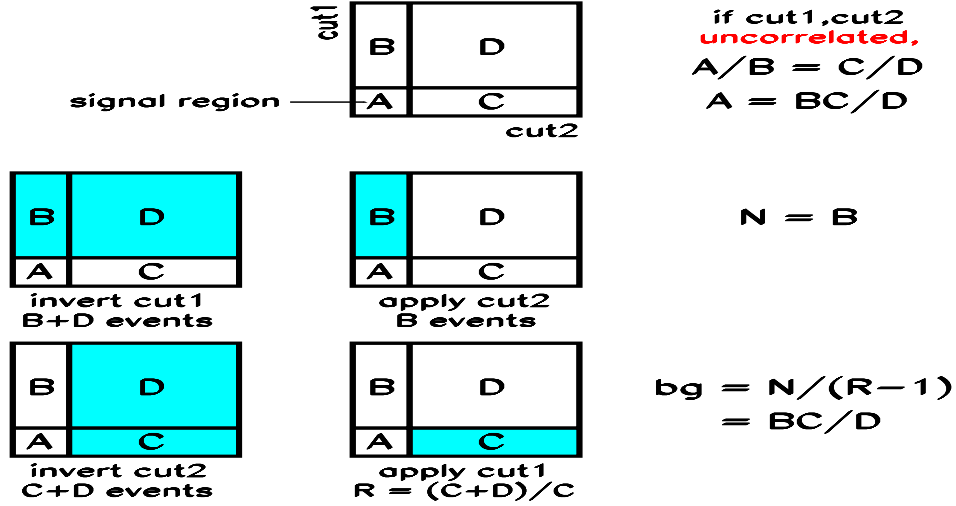


Figure 2: The philosophy of bifurcated analysis.

energy loss in the sub-detectors before entering the RS, the range and kinetic energy resolutions are measured to be $\sigma_R/R \sim 2.9\%$ and $\sigma_E/\sqrt{E(\text{GeV})} \sim 1.0\%$, respectively. A unique feature for the RS is a measurement of the $\pi^+ \rightarrow \mu^+ \rightarrow e^+$ decay sequence from the TDs in the range stack module in which the π^+ comes to rest. The decay sequence observation is a powerful tool in identifying a charged pion. Muon rejection from this information can reach about 10^5 . This cut is independent of the π^+/μ^+ separation using another cut on the range and momentum correlation for different particles, where the π^+/μ^+ separation is more than 3σ .

The outermost detectors are the barrel and end-cap photon vetoes. Together with the lead glass beam counter and additional calorimeters for filling minor openings along the beam direction, they provide a 4π solid angle for detecting photon activity.

3 Background study

The study of $K^+ \rightarrow \pi^+ \nu \bar{\nu}$ adopts the technique of blind analysis, in which selection criteria (cuts) are designed from a study of background samples to avoid bias. Before looking into the signal region (“opening the box”), background levels are estimated using the knowledge outside the signal region. Cuts are designed in such a way to bring the background to the 0.1 event level.

To get a reliable background estimate, a so-called bifurcated analysis is conducted. The philosophy of this method can be illustrated in Figure 2. Experimentally, two uncorrelated cuts giving large background rejection are selected to perform this bifurcated analysis. Based on the event numbers in region C, B and D, the background level in signal region A can be estimated if these two cuts are uncorrelated. The cuts used for the bifurcated analyses are listed in Table 1. In the $\pi^+ \nu \bar{\nu}$ analysis, the $\pi^+ \pi^0$ and $\mu^+ \nu_\mu(\gamma)$ are the two major backgrounds. Since kinematic cuts are based the measurements of the range, kinetic energy and momentum, which are independent of the detection of photon activity and the particle ID using the TD information for recognizing the $\pi^+ \rightarrow \mu^+ \rightarrow e^+$ decay sequence, the bifurcated analyses can be performed between them. To check if they are uncorrelated, a so-called outside-the-box study is conducted by loosening the two cuts and checking if the background level estimated is consistent with the observed.

In estimating background level, $\pi^+ \nu \bar{\nu}$ data are divided into 1/3 and 2/3 samples. The 1/3

Table 1: Cuts used in the bifurcated analyses for the background.

Background	CUT1	CUT2
$\pi^+\pi^0$	Photon veto	Kinematic cuts
$\mu^+\nu_\mu(\gamma)$	RS TD PID	Kinematic cuts
1 beam bkg	Target timings	B4 dE/dx cuts
2 beam bkg	BWPC cuts	B4 2-hit cuts

Table 2: Background estimates for 1995-97 and 1998 data.

Background	1995-7	1998
$\pi^+\pi^0$	0.0216 ± 0.0050	$0.0120^{+0.0031}_{-0.0042}$
$\mu^+\nu_\mu$		0.0092 ± 0.0067
$\mu^+\nu_\mu\gamma$		0.0245 ± 0.0155
$\mu^+\nu_\mu(\gamma)$	0.0282 ± 0.0098	$0.0337^{+0.0435}_{-0.0240}$
1 beam bkg	0.0054 ± 0.0042	0.0039 ± 0.0012
2 beam bkg	0.0157 ± 0.0149	0.0004 ± 0.0001
CEX	0.0096 ± 0.0068	$0.0157^{+0.0050}_{-0.0044}$
Total	0.0804 ± 0.0201	$0.0657^{+0.0438}_{-0.0248}$

sample is used for cuts tuning and initial background evaluation. When the background levels are satisfactory, all the cuts are applied to the 2/3 sample and the background levels are re-estimated. If all cuts are set without bias, the background level from the 1/3 and 2/3 samples should be consistent.

When the checks on the correlation of the two cuts in the bifurcated analysis and the consistency of background estimates between 1/3 and 2/3 sample were performed, no correlations or inconsistencies were observed. The final background estimates using the 2/3 sample are given in Table 2. The charge exchange background estimate is from Monte Carlo. The kaon regeneration rate and beam profile are from the actual measurement using data for the process of $K^+n \rightarrow K_S^0p, K_S^0 \rightarrow \pi^+\pi^-$.

4 Search for signal

Since the background level of 0.15 event estimated for the full E787 data is small, satisfying the single event search in the signal region, the box is opened. Figure 3 shows the range versus kinetic energy for the events surviving all the selection criteria. The box indicated by the solid lines depicts the signal search region. Two signal events are found inside this signal region and the events outside this box are from the $K^+ \rightarrow \pi^+\pi^0$ background due to photons escaping detection. Detailed studies of the candidate events as well as a signal probability study showed that they are consistent with the signature of $K^+ \rightarrow \pi^+\nu\bar{\nu}$.

The E787 experiment can also perform a search below the kinematic peak of the decay $K^+ \rightarrow \pi^+\pi^0$. The study shows the search in this region is limited by the background from $K^+ \rightarrow \pi^+\pi^0$, which should be improved in the ongoing E949 experiment by increasing the photon veto capability.

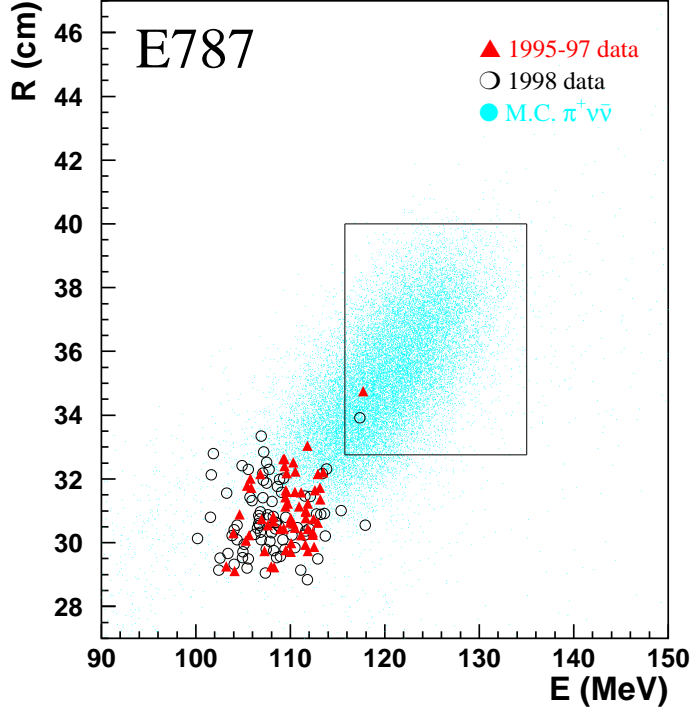


Figure 3: Range versus kinetic energy distribution for all E787 data with all cuts applied except for the range and kinetic energy cuts.

5 Acceptance and branching ratio

The acceptance is estimated using $\mu^+\nu_\mu$, $\pi^+\pi^0$, and π^+ -scattering monitor samples taken simultaneously with the $\pi^+\nu\bar{\nu}$ trigger and by means of a Monte Carlo $\pi^+\nu\bar{\nu}$ sample. Table 3 gives the acceptances for each cut category and the final acceptance. The acceptances for $\pi^+\nu\bar{\nu}$ phase space, solid angle acceptance and π^+ nucleus interaction are estimated using Monte Carlo. Also given are the total K^+ triggers and the corresponding branching ratios assuming no background. The validity is checked against the branching ratio of $K^+ \rightarrow \pi^+\pi^0$ as given below

$$\begin{aligned} \text{Br}(K^+ \rightarrow \pi^+\pi^0) &= 0.208 \pm 0.003_{stat.} \text{ (1995-97)} \\ &= 0.217 \pm 0.003_{stat.} \text{ (1998)} \\ &= 0.212 \pm 0.001 \text{ (PDG)} \end{aligned}$$

The acceptances of the $K^+ \rightarrow \pi^+\nu\bar{\nu}$ and $K^+ \rightarrow \pi^+\pi^0$ decays should differ only in the decay phase space. Agreement with the PDG value is observed.

To combine searches with small statistics for both signal and background level, a statistical analysis⁸ is performed giving the final branching ratio measurement on $K^+ \rightarrow \pi^+\pi^0$ from E787:

$$\text{Br}(K^+ \rightarrow \pi^+\nu\bar{\nu}) = 1.57_{-0.82}^{+1.75} \times 10^{-10}$$

Assuming unitarity, $\bar{m}_t(m_t) = 166 \pm 5 \text{ GeV}/c^2$, $M_W = 80.41 \text{ GeV}/c^2$ and $V_{cb} = 0.041 \pm 0.002$, one can derive the constraint

$$0.007 < |V_{td}| < 0.030 \text{ (68\% C.L.)},$$

without requiring any knowledge of V_{ub} or ϵ_K .

6 Conclusion

The E787 experiment has pursued a decade long search for the rare kaon decay to $\pi^+\nu\bar{\nu}$ with two signal events observed. The branching ratio is measured to be $1.57_{-0.82}^{+1.75} \times 10^{-10}$. The

Table 3: Acceptance study for $K^+ \rightarrow \pi^+ \nu \bar{\nu}$

Category	1995-97	1998
K^+ stop efficiency	0.704	0.702
K^+ decay after 2 ns	0.850	0.851
$\pi^+ \nu \bar{\nu}$ phase space	0.155	0.136
Solid angle acceptance	0.407	0.409
π^+ nucl. interaction	0.513	0.527
Reconstruction efficiency	0.959	0.969
Other kinematic constraints	0.665	0.554
$\pi^+ \rightarrow \mu^+ \rightarrow e^+$ decay acc.	0.306	0.392
Beam and target analysis	0.699	0.706
Accidental loss	0.785	0.751
Total acceptance	0.0021	0.0020
Total K^+ triggers ($\times 10^{12}$)	3.2	2.7
$\text{Br}(K^+ \rightarrow \pi^+ \nu \bar{\nu}) (\times 10^{-10})$	$1.5^{+3.5}_{-1.2}$	$1.9^{+4.4}_{-1.5}$

central value is a factor of two larger than what the Standard Model predicts, though the large uncertainty prevents any solid conclusion on possible new physics. It is expected that the ongoing E949 experiment, which continues the study of the $K^+ \rightarrow \pi^+ \nu \bar{\nu}$ decay at BNL will be able to collect 5 times more statistics and provide a critical test on the Standard Model.

References

1. Giancarlo D'Ambrosio and Gino Isidori, Phys.Lett. B530 (2002) 108.
2. A.J. Buras and R. Fleischer, hep-ph/9704376.
3. Gino Segrè, Phys.Rev. D61 (2000) 077301; S. Fajfer, Nuovo Cim. A110 (1997) 397; C.Q. Geng *et al.*, Phys. Rev. D54 (1996) 877; M. Lu and M.B. Wise, Phys. Lett. B324 (1994) 461.
4. S. Adler *et al.*, Phys. Rev. Lett. 84, (2000) 3768; S. Adler *et al.*, Phys. Rev. Lett. 79, (1997) 2204.
5. S. Adler *et al.*, Phys. Rev. Lett. 88, (2001) 041803.
6. M.S. Atiya *et al.*, Nucl. Inst. and Meth. A321 (1992) 129; E. W. Blackmore *et al.*, Nucl. Inst. and Meth. A404 (1998) 295; I.-H. Chiang *et al.*, IEE Trans. Nucl. Sci. NS-42 (1995) 394; T.K. Komatsubara *et al.*, Nucl. Inst. and Meth. A404 (1998) 315; M. Kobayashi *et al.*, Nucl. Inst. and Meth. A337 (1994) 335; D.A. Bryman *et al.*, Nucl. Inst. and Meth. A396 (1997) 394; M. Burke *et al.*, IEEE Trans. Nucl. Sci. NS-41 (1994) 131; C. Witzig and S. Adler, Real-Time Comput. Appl. (1993) 123; S. Adler, Intl. Conf. Electr. Part. Phys. (1997) 133; C. Zein *et al.*, Real-Time Comput. Appl. (1993) 103.
7. S. Adler *et al.*, hep-ex/0201037.
8. T. Junk, NIM A434 (1999) 435.